

Quantum-Electrodynamical Time-Dependent Density Functional Theory Description of Molecules Interacting with Light

Yetmgeta Aklilu,¹ Tiany Yang,¹ Cody Covington,² and Kálmán Varga^{1,*}

¹*Department of Physics and Astronomy, Vanderbilt University, Nashville, Tennessee, 37235, USA*

²*Department of Chemistry, Austin Peay State University, Clarksville, USA*

We study light-mediated interactions between spatially separated molecules using real-time quantum electrodynamical time-dependent density functional theory based on the Pauli–Fierz Hamiltonian. An ultrashort delta-kick excitation selectively perturbs a single molecule, while a second, distant molecule remains initially unexcited. In free space, the excitation stays localized and no response is observed in the second molecule. In contrast, when both molecules are coupled to the same cavity mode, the initial excitation induces coherent dynamics in the distant molecule through the shared quantized electromagnetic field.

I. INTRODUCTION

Cavity quantum electrodynamics (cavity QED) explores how quantized electromagnetic fields inside optical resonators reshape atomic and molecular behavior. When molecules are placed between mirrors, the vacuum field enhances or suppresses spontaneous emission, modifies energy landscapes, and—in strong coupling regimes—creates polaritonic states that can redirect chemical reactivity and generate new spectroscopic routes [1–4].

Recent reviews span quantum optics, chemistry, and materials science [2–5]. Ebbesen and collaborators highlight how strong coupling reshapes chemical landscapes [1, 6], while Rubio surveys theoretical methods for light-matter hybridization [2, 4]. DePrince summarizes advances in electronic-structure methods for QED chemistry [7, 8], and Basov provides a materials perspective [5]. Together, these reviews reflect the increasingly interdisciplinary reach of cavity QED [8–45].

In cavity QED, two spatially separated atoms (or molecules) can interact over distances far beyond their bare dipole–dipole range because they both couple to the same quantized cavity mode. In the dispersive regime, virtual photon exchange generates effective spin–spin or exciton–exciton couplings that can be engineered to entangle well-separated atom pairs and control their energy-level structure [46, 47]. Experiments and theory now show that this photon-mediated coupling can hybridize distant molecules into “optical bonds,” where individual emitters share delocalized polaritonic states via a common microcavity mode [38]. Real-time simulations of strongly coupled electron–photon dynamics reveal how energy is redistributed between matter and light degrees of freedom during such processes, highlighting the role of polariton formation, dephasing, and dissipation in setting the strength and coherence of inter-atomic interactions [48, 49].

From a more general perspective, off-resonant coupling to the cavity background field can induce long-range,

cavity-mediated interactions between low-energy excitations even when no real photons are present, providing a unifying framework for photon-induced modifications of collective phases and transport [22, 50]. Complementary numerical studies of photon-mediated energy transfer show that the cavity can substantially enhance or suppress transfer efficiencies between atoms and molecules, depending on spectral detuning and spatial configuration [51, 52]. At the many-body level, these mechanisms give rise to cavity-enhanced energy transport in extended molecular systems, where excitations delocalize over many emitters and propagate via polaritonic channels that can span micrometer scales [50, 53]. Together, these works establish that in appropriately designed cavities, “light-induced” interactions are not a small perturbation but a powerful resource for tailoring how two (or many) atoms talk to each other through the shared electromagnetic vacuum.

The Pauli–Fierz (PF) Hamiltonian provides a rigorous and gauge-invariant formulation of the interaction between nonrelativistic charged matter and the quantized electromagnetic field [54, 55]. It constitutes the fundamental starting point for a wide range of theoretical and computational approaches in cavity quantum electrodynamics (QED) [56, 57], enabling a consistent treatment of light–matter coupling across different gauges and levels of approximation. Owing to the explicit coupling between electronic and photonic degrees of freedom, the PF Hamiltonian leads to a substantially enlarged Hilbert space, rendering its exact solution generally intractable for realistic many-body systems.

In practice, this complexity is addressed by adopting either wave-function-based or density-based approaches. Wave-function-based methods explicitly represent the coupled electron–photon state in a tensor-product Hilbert space and allow for systematic improbability and high accuracy, albeit at a steep computational cost [38, 58]. In contrast, density-based approaches, most notably quantum electrodynamical density functional theory (QED-DFT), reformulate the PF problem in terms of reduced variables, yielding coupled auxiliary equations for matter and photon fields that are computationally more tractable for extended systems [56, 59].

* kalman.varga@vanderbilt.edu

Wavefunction-based cavity QED approaches explicitly construct correlated electron–photon states in a tensor-product Hilbert space composed of an electronic many-body basis and a photonic Fock basis. Within this framework, the full PF Hamiltonian is treated variationally or through systematic many-body expansions, enabling an accurate and nonperturbative description of strong light–matter coupling and photon dressing effects. Representative methods include quantum electrodynamical Hartree–Fock (QED-HF) [60], coupled-cluster generalizations such as QED-CC and equation-of-motion QED-CC [58, 61], and multireference approaches like QED complete-active-space configuration interaction (QED-CASCI) [62]. In addition, explicitly correlated stochastic variational methods have been developed to capture electron–photon correlations beyond standard orbital-based expansions [63, 64]. These wavefunction-based methods are systematically improvable and can achieve benchmark-level accuracy for ground and excited polaritonic states. However, their computational cost grows steeply with the number of electronic degrees of freedom and photon modes, as the combined electron–photon Hilbert space scales exponentially. This limits their applicability to relatively small molecular systems and few-mode cavities.

Density-based methods, most notably quantum electrodynamical density functional theory (QED-DFT), reformulate the PF problem in terms of coupled electron and photon densities rather than explicit many-body wavefunctions. In this approach, the interacting electron–photon system is mapped onto auxiliary Kohn–Sham electrons coupled to quantized or classical Maxwell-like equations for the photon modes [56, 65].

The resulting QED-Kohn–Sham equations retain the favorable scaling of conventional electronic DFT while incorporating light–matter interactions through effective electron–photon exchange–correlation functionals [66]. This framework enables simulations of realistic molecular and condensed-phase systems in optical cavities, spanning regimes from weak to strong coupling [59].

Practical implementations often employ reduced cavity descriptions or effective models, such as single-mode Rabi or Dicke Hamiltonians, to capture dominant photonic effects at low computational cost [35, 67]. While QED-DFT is computationally efficient and scalable, its predictive accuracy depends critically on the development of reliable exchange–correlation approximations capable of describing nonclassical electron–photon correlations.

To describe realistic cavity QED systems within the Pauli–Fierz framework, further physically motivated approximations are typically introduced in order to render the problem computationally tractable. One central simplification is the dipole (long-wavelength) approximation, which exploits the separation of length scales between the spatial extent of the matter subsystem and the wavelength of the relevant cavity modes. When the electronic system is localized on a length scale much smaller than the cavity wavelength, the spatial dependence of the elec-

tromagnetic mode functions can be neglected across the matter region, and the vector potential may be evaluated at a fixed reference position. As a result, the light–matter interaction reduces to a coupling between the total electric dipole moment of the matter system and the quantized field amplitude, while preserving gauge invariance at the level of the full Pauli–Fierz Hamiltonian [55, 56].

A second widely employed approximation is the truncation of the electromagnetic field to a finite number of cavity modes, often to a single resonant mode that dominates the light–matter interaction. This truncation is physically justified when the cavity features a well-isolated resonance with a large quality factor and when off-resonant modes are energetically separated and weakly populated. However, care must be taken, as a naive mode truncation can violate gauge invariance and lead to unphysical results, such as spurious ground-state instabilities or incorrect light–matter decoupling limits. A consistent single-mode description therefore requires retaining all gauge-related terms generated by the truncation, including diamagnetic contributions and self-polarization terms, ensuring that physical observables remain gauge invariant [56, 59, 68]. Under these conditions, the single-mode Pauli–Fierz Hamiltonian provides a controlled and widely used effective model for realistic cavity QED systems.

Importantly, no physical cavity is strictly single mode; rather, this approximation is justified when one cavity mode dominates the dynamics over all relevant energy and time scales [1, 69, 70]. Such conditions are realized in a variety of experimental platforms. In Fabry–Pérot microcavities, a small mirror separation leads to a large free spectral range, allowing a single standing-wave mode to be spectrally isolated from neighboring longitudinal and transverse modes. Photonic crystal nanocavities provide an even stronger form of modal confinement, where a localized defect mode appears inside a photonic bandgap, yielding ultra-small mode volumes and strong light–matter coupling [71]. In the microwave domain, circuit QED architectures achieve exceptionally clean single-mode behavior through large mode spacings and low dissipation [72, 73]. Plasmonic nanocavities, while intrinsically lossy, can also be described in terms of an effective single dominant resonance when dissipation and non-Hermitian effects are properly accounted for [69, 70].

In this work, we present a real-time, first-principles investigation of light-mediated interactions between spatially separated molecules using time-dependent quantum electrodynamical density functional theory (QED-TDDFT) in the velocity gauge. Our approach combines a Pauli–Fierz Kohn–Sham formulation with a tensor-product representation of electronic real-space orbitals and photonic Fock states, enabling explicit simulation of coupled electron–photon dynamics beyond perturbation theory. The electromagnetic field is treated within a consistent single-mode approximation, retaining both paramagnetic and diamagnetic couplings to preserve gauge invariance [74].

We use a delta-kick excitation to selectively excite only one molecule in a system of two widely separated molecules, followed by real-time propagation of the coupled electron–photon system. The delta kick represents an ultrashort laser pulse that instantaneously imparts momentum to the electrons of the targeted molecule while leaving the second molecule completely unperturbed at the initial time. This protocol allows us to unambiguously isolate and identify the mechanism by which excitation can be transferred between distant molecules.

Our results demonstrate a striking contrast between vacuum and cavity environments. In the absence of light–matter coupling, excitation remains strictly localized: the molecule subjected to the delta kick exhibits dipole oscillations, while the second molecule—being far beyond the range of direct intermolecular interactions—remains entirely unexcited. In sharp contrast, when both molecules are coupled to the same cavity mode, the initially excited molecule generates a cross-coupling via the shared the photon field, which then exerts a back action on the second, distant molecule. After a short transient, the unexcited molecule begins to oscillate, eventually synchronizing its dipole motion with that of the initially perturbed molecule. This behavior provides direct, real-time evidence of photon-mediated excitation transfer between distant molecular subsystems [50–52].

By analyzing the time evolution of molecular dipoles, photon occupation numbers, photon coordinates, and charge-density rearrangements, we show that the cavity mode acts as a dynamical communication channel that converts a strictly local excitation into a collective response. Importantly, this effect does not rely on near-field Coulomb interactions, molecular overlap, or classical radiation fields; it arises solely from the coherent coupling of both molecules to the quantized cavity mode. The phenomenon persists across different molecular species (formaldehyde, HF, CO, and mixed dimers), and its strength and symmetry depend sensitively on molecular orientation and field polarization [38, 75].

Overall, this work establishes a clear and physically transparent picture of how ultrashort optical excitation of a single molecule can trigger coherent dynamics in a distant, initially inactive molecule via quantized light. Beyond its fundamental significance, this mechanism opens new possibilities for cavity-controlled energy transport, molecular synchronization, and nonlocal manipulation of molecular excitations on ultrafast timescales [1, 4].

II. FORMALISM

The Pauli–Fierz Hamiltonian provides a gauge-invariant description of nonrelativistic charged matter interacting with quantized electromagnetic fields. In the velocity (Coulomb) gauge, the separation between instantaneous Coulomb interactions and dynamical photon-mediated interactions is explicit. This makes the velocity gauge particularly well suited for discussing

truncations of the photonic Hilbert space, such as the single-mode approximation commonly used in cavity quantum electrodynamics.

A. Pauli–Fierz Hamiltonian in Velocity Gauge

We work in the Coulomb gauge, $\nabla \cdot \hat{\mathbf{A}}(\mathbf{r}) = 0$, and consider nonrelativistic electrons of charge $-e$ and mass m interacting with the quantized electromagnetic field.

The full Pauli–Fierz Hamiltonian reads

$$\hat{H} = \sum_i \frac{1}{2m} \left[\hat{\mathbf{p}}_i + e\hat{\mathbf{A}}(\hat{\mathbf{r}}_i) \right]^2 + \hat{V}_{\text{ext}} + \hat{V}_{\text{Coul}}^{\parallel} + \hat{H}_{\text{EM}}, \quad (1)$$

where $\hat{\mathbf{p}}_i = -i\hbar\nabla_i$ is the canonical momentum, \hat{V}_{ext} includes nuclei–electron interactions and any external scalar potentials. The instantaneous longitudinal Coulomb interaction,

$$\hat{V}_{\text{Coul}}^{\parallel} = \frac{1}{2} \int d\mathbf{r} d\mathbf{r}' \frac{\hat{\rho}(\mathbf{r})\hat{\rho}(\mathbf{r}')}{4\pi\varepsilon_0|\mathbf{r} - \mathbf{r}'|}, \quad (2)$$

with the electron charge density operator

$$\hat{\rho}(\mathbf{r}) = -e \sum_i \delta(\mathbf{r} - \hat{\mathbf{r}}_i). \quad (3)$$

This term is *independent of the transverse vector potential* and is fixed by Gauss's law. It must not be altered when truncating the photon field [76].

The transverse vector potential is expanded in cavity modes:

$$\hat{\mathbf{A}}(\mathbf{r}) = \sum_{\alpha} \sqrt{\frac{\hbar}{2\varepsilon_0\omega_{\alpha}}} \mathbf{f}_{\alpha}(\mathbf{r}) (\hat{a}_{\alpha} + \hat{a}_{\alpha}^{\dagger}), \quad (4)$$

where $\mathbf{f}_{\alpha}(\mathbf{r})$ are real transverse mode functions satisfying the cavity boundary conditions and normalization (e.g. $\int_V d\mathbf{r} |\mathbf{f}_{\alpha}(\mathbf{r})|^2 = 1$). The Hamiltonian of the transverse photon field is defined as

$$\hat{H}_{\text{EM}} = \sum_{\alpha} \hbar\omega_{\alpha} \left(\hat{a}_{\alpha}^{\dagger}\hat{a}_{\alpha} + \frac{1}{2} \right). \quad (5)$$

B. Single–Mode Truncation in Velocity Gauge

A consistent single–mode approximation is obtained by *projecting the transverse vector potential onto one cavity mode $\alpha = c$* :

$$\hat{\mathbf{A}}(\mathbf{r}) \longrightarrow \hat{\mathbf{A}}_c(\mathbf{r}) = \sqrt{\frac{\hbar}{2\varepsilon_0\omega_c}} \mathbf{f}_c(\mathbf{r}) (\hat{a}_c + \hat{a}_c^{\dagger}), \quad (6)$$

and simultaneously truncating the photon Hamiltonian to

$$\hat{H}_{\text{EM}} \longrightarrow \hbar\omega_c \left(\hat{a}_c^{\dagger}\hat{a}_c + \frac{1}{2} \right). \quad (7)$$

No modification is made to the longitudinal Coulomb interaction or to the KS scalar potential V_{KS} .

C. Single-Mode PF-KS Hamiltonian

The single-particle KS Hamiltonian in the single-mode velocity gauge becomes

$$\hat{H}_{\text{KS}} = \frac{1}{2m} \left[-i\hbar\nabla + e\hat{\mathbf{A}}_c(\mathbf{r}) \right]^2 + V_{\text{KS}}(\mathbf{r}, t). \quad (8)$$

Expanding the kinetic term yields

$$\hat{H}_{\text{KS}} = \frac{\hat{\mathbf{p}}^2}{2m} + \frac{e}{m}\hat{\mathbf{p}} \cdot \hat{\mathbf{A}}_c(\mathbf{r}) + \frac{e^2}{2m}\hat{\mathbf{A}}_c^2(\mathbf{r}) + V_{\text{KS}}(\mathbf{r}, t). \quad (9)$$

Both the paramagnetic $\hat{\mathbf{p}} \cdot \hat{\mathbf{A}}_c$ and diamagnetic $\hat{\mathbf{A}}_c^2$ terms must be retained.

D. Dipole (Long-Wavelength) Approximation

Assume the electronic system is localized near a point \mathbf{r}_0 (e.g. the molecular center of mass) within a region of characteristic size ℓ . If the cavity mode varies on a length scale L such that

$$\ell \ll L, \quad (10)$$

then within the matter region the mode profile can be approximated as constant:

$$\mathbf{f}_c(\mathbf{r}) \approx \mathbf{f}_c(\mathbf{r}_0) \equiv \mathbf{f}_c^0. \quad (11)$$

This is the *dipole* or *long-wavelength* approximation.

In this approximation the vector potential becomes spatially uniform over the matter:

$$\hat{\mathbf{A}}_c(\mathbf{r}) \approx \hat{\mathbf{A}}_c(\mathbf{r}_0) = \mathcal{A}_c(\hat{a}_c + \hat{a}_c^\dagger), \quad \mathcal{A}_c \equiv \sqrt{\frac{\hbar}{2\varepsilon_0\omega_c}} \mathbf{f}_c^0. \quad (12)$$

Often one writes $\mathbf{f}_c^0 = \frac{\boldsymbol{\varepsilon}}{\sqrt{V_{\text{eff}}}}$, where $\boldsymbol{\varepsilon}$ is a (unit) polarization vector and V_{eff} is an effective mode volume at \mathbf{r}_0 . Introducing the dimensionless photon coordinate $\hat{q}_c = (\hat{a}_c + \hat{a}_c^\dagger)/\sqrt{2}$, the vector potential becomes spatially uniform,

$$\hat{\mathbf{A}}_c = \sqrt{\frac{\hbar}{\omega_c}} \boldsymbol{\lambda}_c \hat{q}_c, \quad \boldsymbol{\lambda}_c = \frac{\boldsymbol{\varepsilon}_c}{\sqrt{\varepsilon_0 V}}, \quad (13)$$

E. Dipole-Approximate Single-Mode PF-KS Hamiltonian

Inserting Eq. (12) into Eq. (8) yields the dipole-approximate PF-KS single-particle Hamiltonian

$$\hat{H}_{\text{KS}} = \frac{1}{2m} \left[-i\hbar\nabla + e\mathcal{A}_c(\hat{a}_c + \hat{a}_c^\dagger) \right]^2 + V_{\text{KS}}(\mathbf{r}, t). \quad (14)$$

The KS potential is decomposed as

$$V_{\text{KS}}(\mathbf{r}) = V_{\text{H}}[\rho](\mathbf{r}) + V_{\text{XC}}[\rho](\mathbf{r}) + V_{\text{ion}}(\mathbf{r}), \quad (15)$$

with V_{H} the Hartree term, V_{XC} a GGA exchange-correlation functional (e.g., Perdew–Burke–Ernzerhof) [77], and V_{ion} the external ionic potential.

F. Tensor-Product KS Ansatz

We represent the KS orbitals on a tensor-product of real space and photon Fock space. For electronic orbital index m and photon number n ,

$$\Phi_{mn}(\mathbf{r}) = \phi_{mn}(\mathbf{r}) \otimes |n\rangle, \quad n = 0, \dots, N_F, \quad (16)$$

where N_F is the Fock truncation (often $N_F = 1$ for the vacuum plus single-photon sector). In practice, the computational domain of size $N_x \times N_y \times N_z \times N_F$, with (N_x, N_y, N_z) the real-space grid.

Because Fock states are orthonormal, overlaps factorize:

$$\langle \Phi_{mn} | \Phi_{m'n'} \rangle = \langle \phi_{mn} | \phi_{m'n'} \rangle \delta_{nn'}, \quad (17)$$

where the real-space inner product is

$$\langle \phi_{mn} | \phi_{m'n} \rangle = \sum_{i,j,k} \phi_{mn}(x_i, y_j, z_k) \phi_{m'n}(x_i, y_j, z_k). \quad (18)$$

We orthogonalize the real-space components within each photon sector (e.g., Gram–Schmidt) and normalize such that

$$\sum_{n=0}^{N_F} \left\| \hat{\phi}_{mn} \right\|^2 = 1 \quad \forall m. \quad (19)$$

The expansion of the kinetic term in (14) contains the paramagnetic coupling

$$\frac{e}{m} \hat{\mathbf{p}} \cdot \hat{\mathbf{A}} = \frac{e}{m} \sqrt{\frac{\hbar}{\omega_c}} \hat{\mathbf{p}} \cdot \boldsymbol{\lambda}_c \hat{q}_c, \quad (20)$$

and the diamagnetic (seagull) term

$$\frac{e^2}{2m} \hat{\mathbf{A}}^2 = \frac{e^2}{2m} \frac{\hbar}{\omega_c} \boldsymbol{\lambda}_c^2 \hat{q}_c^2. \quad (21)$$

The paramagnetic interaction links photon states that differ by one quantum number ($\Delta n = \pm 1$), while the diamagnetic interaction connects photon states with quantum number changes of $\Delta n = 0, \pm 2$. In the special case where the diamagnetic term couples photon states with identical quantum numbers ($\Delta n = 0$), it behaves analogously to the dipole self-interaction (DSI) found in the length-gauge formulation.

G. Physical quantities

The full KS orbital is

$$|\Phi_m(t)\rangle = \sum_{n=0}^{N_F} \phi_{mn}(\mathbf{r}, t) \otimes |n\rangle. \quad (22)$$

We define the electronic dipole moment operator of the system as

$$\hat{\mathbf{d}} = -e\hat{\mathbf{r}}, \quad (23)$$

where e is the elementary charge and $\hat{\mathbf{r}}$ is the electronic position operator. The total dipole moment (summed over occupied orbitals) is then

$$\mathbf{d}(t) = \sum_{m \in \text{occ}} \langle \Phi_m(t) | \hat{\mathbf{d}} | \Phi_m(t) \rangle. \quad (24)$$

We define the weight of the n -photon sector (summed over orbitals) as

$$P_n(t) = \sum_m \int d\mathbf{r} |\phi_{mn}(\mathbf{r}, t)|^2. \quad (25)$$

For a single photon mode with frequency ω (we drop c in the following) the photon coordinate operator is

$$\hat{q} = \sqrt{\frac{\hbar}{2\omega}} (\hat{a} + \hat{a}^\dagger). \quad (26)$$

The expectation value of the photon coordinate for the KS orbital $|\Phi_m\rangle$ is therefore

$$\begin{aligned} q_m(t) &= \langle \Phi_m(t) | \hat{q} | \Phi_m(t) \rangle \\ &= \sqrt{\frac{\hbar}{2\omega}} \sum_{n=0}^{N_F-1} \sqrt{n+1} (\langle \phi_{mn} | \phi_{mn+1} \rangle + \langle \phi_{mn+1} | \phi_{mn} \rangle) \end{aligned} \quad (27)$$

The total photon-coordinate expectation value is obtained by summing over orbitals,

$$q(t) = \sum_m q_m(t). \quad (28)$$

The photon coordinate depends on the coherence between adjacent photon-number sectors $|n\rangle$ and $|n+1\rangle$, not on the photon-number probabilities $|\phi_{mn}|^2$ alone.

We can also define the energy of system A

$$E_A(t) = \sum_{m \in A} \langle \Phi_m(t) | \hat{H} | \Phi_m(t) \rangle, \quad (29)$$

where the summation includes orbitals belong to system A. This will be used to characterize energy transfer between two molecules. The dipole of a given subsystem can be defined similarly to (24) restricting the summations to the orbitals belonging to A.

H. Time propagation

The real-time evolution of each Kohn–Sham (KS) orbital $\Phi_m(t)$ is governed by the time-dependent Schrödinger equation

$$i\hbar \frac{\partial}{\partial t} |\Phi_m(t)\rangle = \hat{H}_{KS}(t) |\Phi_m(t)\rangle \quad (30)$$

The initial KS orbitals are obtained by minimizing the ground-state Kohn–Sham energy functional defined on the coupled electron–photon Hilbert space. This minimization is carried out using iterative gradient-based

schemes, where the Pauli–Fierz–augmented Hamiltonian is assembled in a tensor-product representation of electronic real-space orbitals and photonic Fock states.

To access excitation spectra, the system is perturbed at the initial time by an impulsive (delta-kick) perturbation. In the velocity gauge, the excitation is implemented via a spatially uniform, time-dependent vector potential,

$$\mathbf{A}(t) = -\kappa \hat{\mathbf{e}} \Theta(t), \quad (31)$$

where κ controls the strength of the perturbation, $\hat{\mathbf{e}}$ is the polarization direction, and $\Theta(t)$ is the Heaviside step function. The associated electric field is given by $\mathbf{E}(t) = -\partial_t \mathbf{A}(t) = \kappa \hat{\mathbf{e}} \delta(t)$.

In the PF Hamiltonian formulated in the velocity gauge, the coupling to the vector potential enters through the minimal-coupling substitution. The action of the delta kick is therefore realized by an instantaneous boost of the electronic momenta. At the level of the KS orbitals, this corresponds to the transformation

$$\Phi_m(0^+) = e^{-i\kappa \hat{\mathbf{e}} \cdot \mathbf{r}} \Phi_m(0^-), \quad (32)$$

which is equivalent, up to a gauge transformation, to the length-gauge formulation. For sufficiently small κ , this procedure excites all dipole-allowed modes simultaneously.

In cavity QED simulations, the velocity-gauge delta kick provides a numerically convenient and gauge-consistent way to initiate coupled electron–photon dynamics, particularly when paramagnetic and diamagnetic light–matter coupling terms are treated explicitly.

The real-time propagation of the Kohn–Sham orbitals is performed using an explicit fourth-order Taylor expansion of the time-evolution operator, a method that has proven robust and efficient for real-space time-dependent density-functional theory and its extensions [78, 79]. The accuracy and stability of this approach rely on a consistent choice of the time step and spatial grid spacing, as discussed in detail in the context of computational nanoscience simulations [80].

Explicitly, the KS orbitals are advanced according to

$$|\Phi_m(t + \Delta t)\rangle = \sum_{k=0}^4 \frac{1}{k!} \left(\frac{i\Delta t}{\hbar} \hat{H}(t) \right)^k |\Phi_m(t)\rangle \quad (33)$$

The numerical accuracy and stability of the propagation require a consistent choice of the time step Δt and the spatial grid spacing Δx . On a real-space grid, the highest kinetic-energy components that can be represented are determined by the grid spacing,

$$E_{\max} \sim \frac{\hbar^2}{2m(\Delta x)^2}. \quad (34)$$

To accurately resolve these components, the time step must satisfy

$$\Delta t \ll \frac{\hbar}{E_{\max}} \sim \frac{2m}{\hbar} (\Delta x)^2. \quad (35)$$

When this condition is fulfilled, the fourth-order Taylor propagator provides stable and accurate real-time dynamics of the KS orbitals in coupled electron–photon systems.

III. RESULTS

A. Nitrobenzene in cavity coupled to light

We computed the ground state of a single Nitrobenzene molecule both in vacuum and within an optical cavity. Following convergence of the ground-state calculation, the system was perturbed by a delta-kick pulse, and the molecular orbitals were propagated in time. Fig. 1 displays the time evolution of the dipole moment for Nitrobenzene, plotted as $d = d(t) - d_0$, where d_0 represents the ground-state dipole moment. Two scenarios are compared: the molecule inside an optical cavity (with light-matter coupling) and the molecule in vacuum (without coupling). The results reveal that cavity coupling substantially amplifies the dipole response. To further illustrate the contrast between these two environments, we analyzed snapshots of the electron density difference, obtained by subtracting the ground-state density from the time-dependent excited-state density. Fig. 2 demonstrates that density oscillations differ markedly between the cavity and vacuum cases. In the cavity, the density oscillations are more pronounced and localized to distinct regions of the molecule. While the oscillations decay over

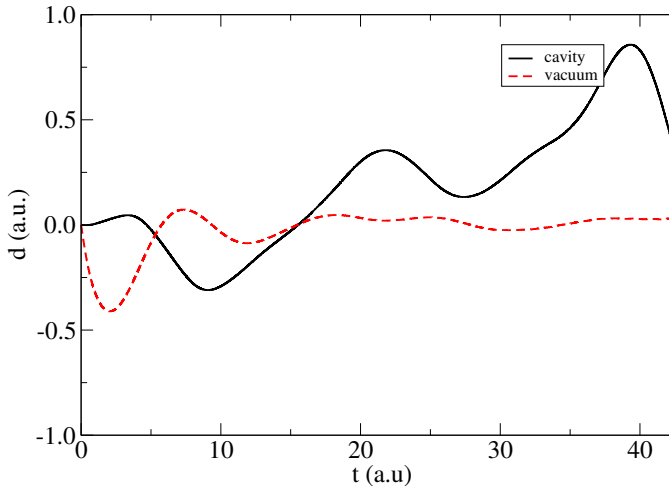


FIG. 1: Temporal dynamics of nitrobenzene's dipole moment. Solid line: cavity-coupled molecule; dashed line: uncoupled molecule in vacuum (magnified by 100 for clarity). $\lambda = 0.005$ a.u. and $\omega = 0.289$ a.u. is used in the calculations.

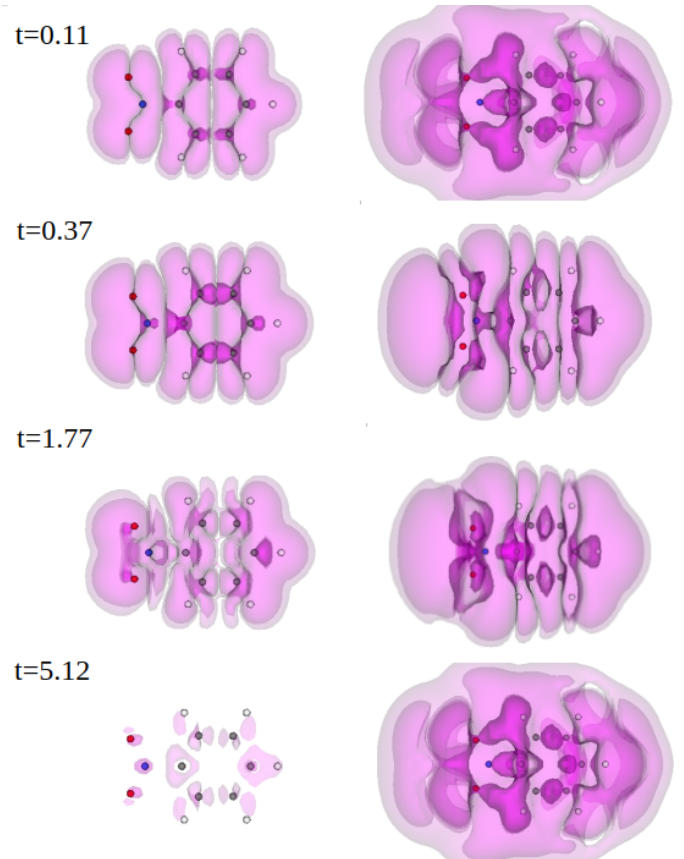


FIG. 2: Snapshots of the charge density difference between the excited state and the ground state. Left panel: molecule in vacuum; right panel: molecule in an optical cavity. All parameters are identical to those used in Fig. 1. The three shades of magenta represents values of $-0.00002, -0.00001, 0.00002$ electrons/ Δx^3 ranging from the lightest to the darkest.

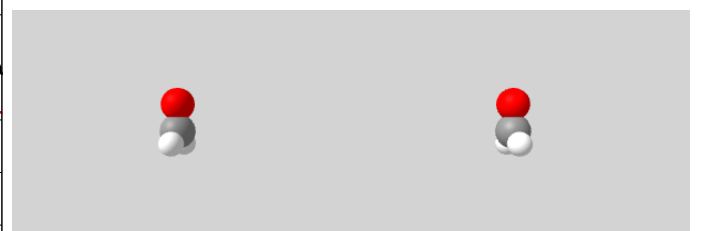
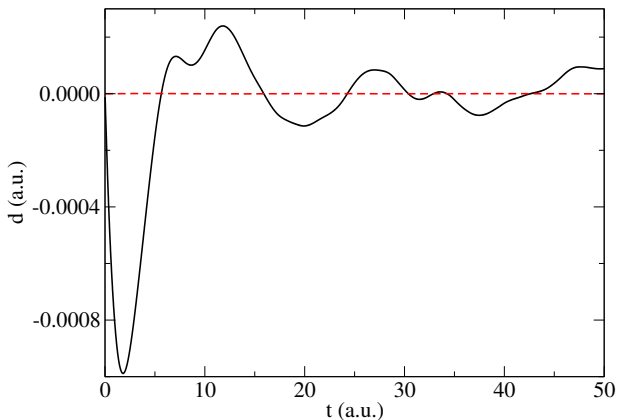


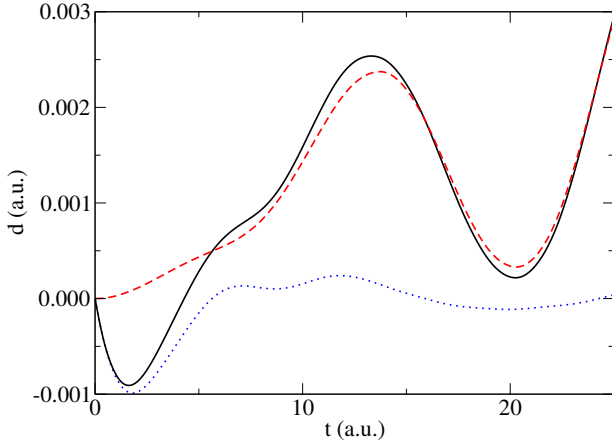
FIG. 3: Formaldehyde dimer configuration: cavity frequency $\omega = 0.289$, light-matter coupling strength $\lambda = 0.005$. The light polarization vector is aligned along the O-C bond direction of each molecule, with the O-C axes positioned perpendicular to the z-axis that connects the two carbon centers.

B. Two formaldehyde molecules coupled by light

Next, we examine the light-matter interaction between two spatially separated molecules. The system consists



(a) Time evolution of dipole moments following delta



(b) Dipole moment dynamics with light-mediated coupling after selective delta kick excitation of the left molecule: left molecule (solid black), right molecule (dashed red). The blue dotted line shows the uncoupled evolution of the left molecule for comparison, identical to the black curve in the previous figure.

FIG. 4: Temporal evolution of dipole moment changes relative to ground state values for the formaldehyde dimer.

of two formaldehyde molecules separated by a large distance (30 a.u.) (see Fig. 3) such that their direct interaction (without light coupling) is negligible. Formaldehyde has a substantial dipole moment of 2.33 Debye, enabling strong light coupling. The left molecule is selectively excited with a delta kick, and the system dynamics are time-propagated. In the first case, where molecules are not coupled to light, Fig. 4a demonstrates that only the excited left molecule's dipole moment evolves, while the right molecule's dipole remains unchanged at zero. Fig 4b compares the dipole dynamics when molecules are light-coupled, with only the left molecule receiving delta kick excitation. Initially, the left molecule's dipole begins oscillating due to the excitation, while the un-

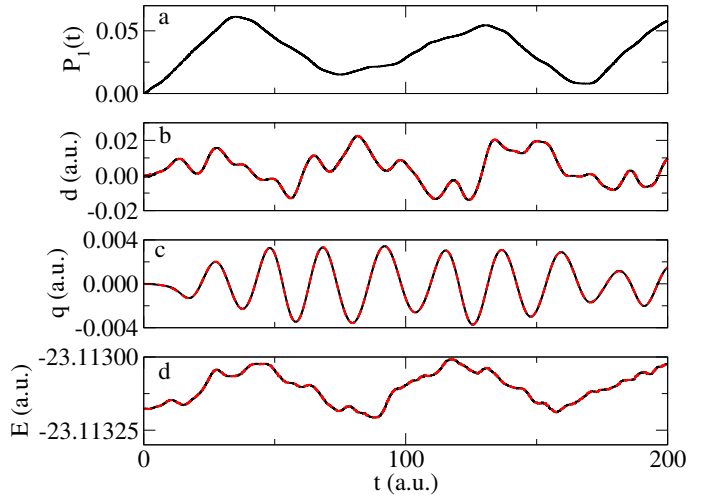


FIG. 5: Temporal evolution of (a) photon occupation number P_1 of the $|1\rangle$ space, (b) dipole moment, (c) photon coordinate and (d) energies of the formaldehyde dimer. The solid black line shows the dynamics of the left, kicked molecule, the dashed red line represents the right initially unperturbed system.

excited right molecule's dipole remains near zero for the first 2-3 atomic units of time. After approximately 5 a.u., the right molecule's dipole also begins to oscillate, closely following the left molecule's behavior. For comparison, this figure includes the uncoupled left molecule evolution (blue dotted line). Initially, the coupled and uncoupled systems behave similarly, but after 5 a.u., light-mediated coupling causes the systems to diverge.

Fig. 5 extends the coupled dynamics over a longer time period, revealing that after the initial few atomic units, the two molecular dipoles evolve nearly identically, demonstrating strong synchronization through light-mediated coupling. The figure illustrates the temporal evolution of the photon occupation number (Fig.5a), dipole moment (Fig.5b), photon coordinate (Fig.5c), and energies (Fig.5d) as the formaldehyde dimer molecules move in a concerted, identical manner. An interesting observation is that the photon occupation number and photon coordinate, though related, oscillate with very different periods. The dipole moment—a real-space variable—also oscillates, but its behavior differs from both quantities. The energy, however, shows an oscillation pattern more similar to that of the photon occupation number. This can be easily understood: the photon occupation corresponds to population changes between the zero-photon and one-photon states, which have different energies. Consequently, the total energy oscillates synchronously with these occupation changes.

Fig. 6 shows temporal snapshots of charge oscillations for both molecules. At early times, only the perturbed molecule displays appreciable oscillations, while charge rearrangement gradually builds up on the second molecule. Eventually, the charge oscillations synchro-

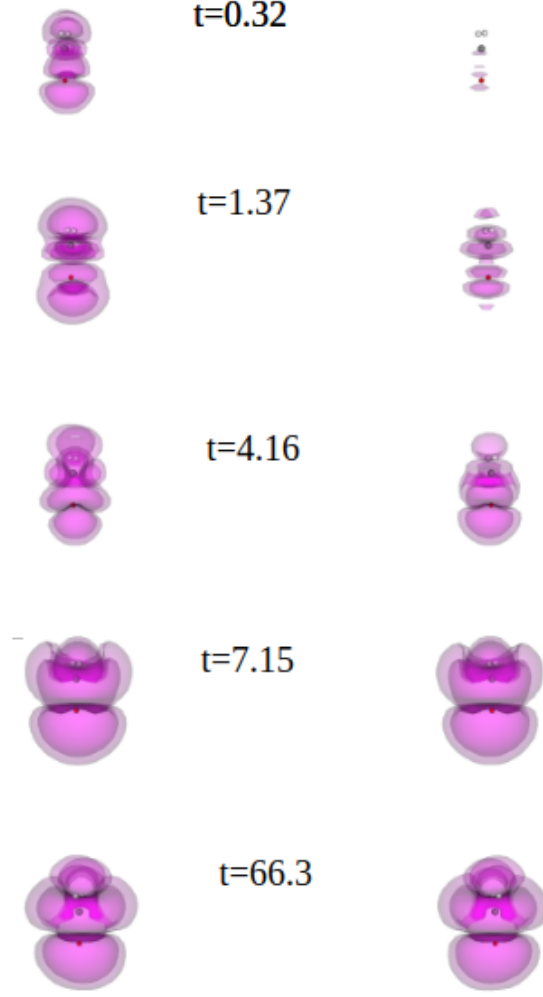


FIG. 6: Snapshots of the charge density difference between the excited state and the ground state for the COH_2 molecule. The left molecule is excited with a delta kick perturbation. $\lambda = 0.005$ a.u. and $\omega = 0.289$ a.u. is used in the calculations. The three shades of magenta represents values of $-0.00005, -0.0002, 0.00005$ electrons/ Δx^3 ranging from the lightest to the darkest.

nize, with both molecules oscillating identically, as evidenced by the dipole oscillation (Fig. 5b).

C. Two HF molecules coupled by light

Next, we present a similar calculation using two spatially separated HF molecules. The molecules are aligned parallel to each other and to the x-axis, with a separation of 30 a.u. along the perpendicular z-direction. The electromagnetic field is polarized along the x-axis, parallel to the molecular axes. Fig. 7 displays the occupation of the $|1\rangle$ Fock state and the time evolution of

the dipole moment. As observed in the formaldehyde case, the dipole moments of both molecules oscillate synchronously after an initial transient period during which the perturbed molecule induces charge oscillations in the second molecule. Here, the dipole oscillations exhibit periodic sinusoidal behavior, and the Fock state occupation follows this oscillatory pattern. This contrasts sharply

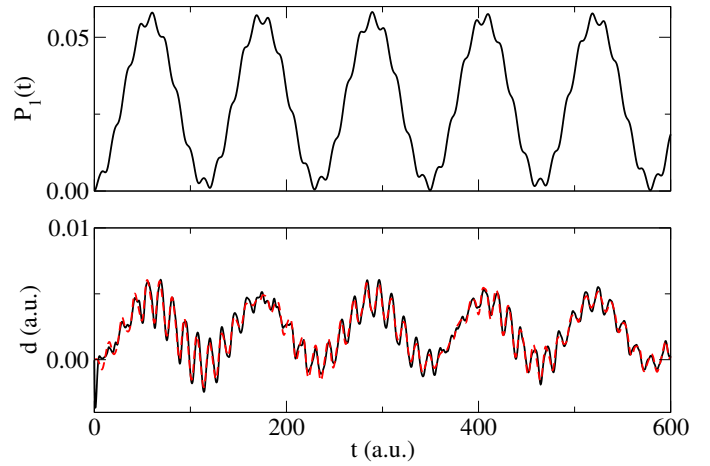


FIG. 7: Occupation of the $|1\rangle$ Fock space and the change of the dipole moment as the function of time. The solid black line shows the dipole of the molecule which was perturbed by a delta kick excitation, the red dashed line shows the dipole of the second molecule. $\lambda = 0.01$ a.u. and $\omega = 0.467$ a.u. is used in the calculations.

The coupling between the two molecules is highly sensitive to their relative orientation and the polarization of the incident light. Fig. 8 illustrates the dipole moment evolution when the molecule excited by the delta kick is aligned parallel to the light polarization—identical to the previously discussed parallel configuration—while the second unperturbed molecule is oriented along the z-axis, perpendicular to the first molecule. The dipole moment of the first molecule exhibits the same temporal behavior as before, whereas the dipole moment of the second molecule remains nearly constant over time. Fig. 8 also displays the occupation dynamics of the $|1\rangle$ Fock state. While the occupation pattern resembles that of the parallel case, its amplitude is reduced by half due to the negligible contribution from the second molecule.

The orientation dependence is further demonstrated in Fig. 9. In this configuration, the two molecules are aligned antiparallel to each other, with their molecular axes perpendicular to the field polarization. The occupation of the $|1\rangle$ Fock state remains largely consistent with the parallel case (Fig.9a); however, the dipole moments now oscillate synchronously in opposite directions (Fig.9b). The photon coordinates also oscillate in the opposite direction, but with different amplitudes (Fig.9c).

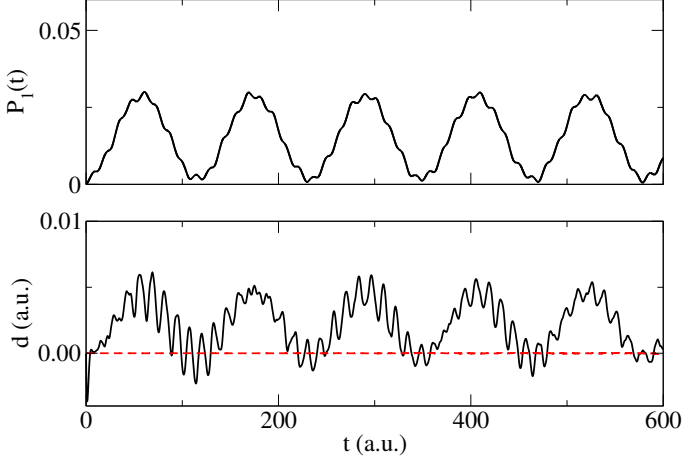


FIG. 8: Two HF molecules oriented perpendicularly. Temporal evolution of (a) photon occupation number, (b) dipole moment, (c) photon coordinate and (d) energies of the formaldehyde dimer. The solid black line shows the dynamics of the left, kicked molecule, the dashed red line represents the right initially unperturbed system. $\lambda = 0.01$ a.u. and $\omega = 0.467$ a.u. is used in the calculations.

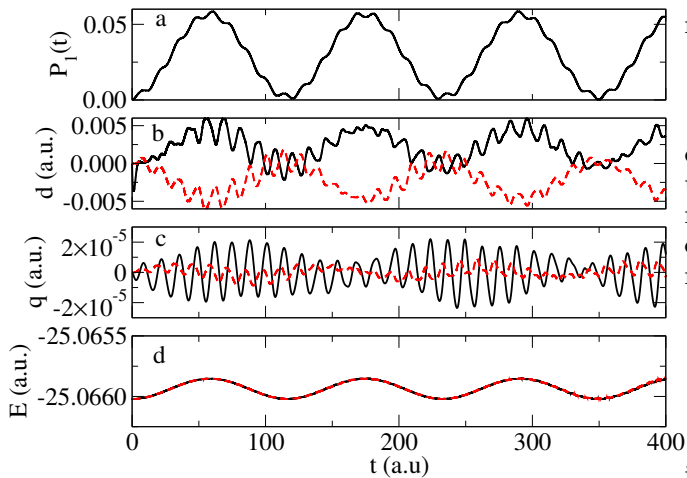


FIG. 9: Two HF molecules oriented antiparallel. Temporal evolution of (a) photon occupation number, (b) dipole moment, (c) photon coordinate and (d) energies of the formaldehyde dimer. The solid black line shows the dynamics of the left, kicked molecule, the dashed red line represents the right initially unperturbed system. $\lambda = 0.01$ a.u. and $\omega = 0.467$ a.u. is used in the calculations.

Fig. 10 displays snapshots of the charge density variations for the antiparallel-oriented HF molecules. As observed in the formaldehyde case, excitation initially occurs

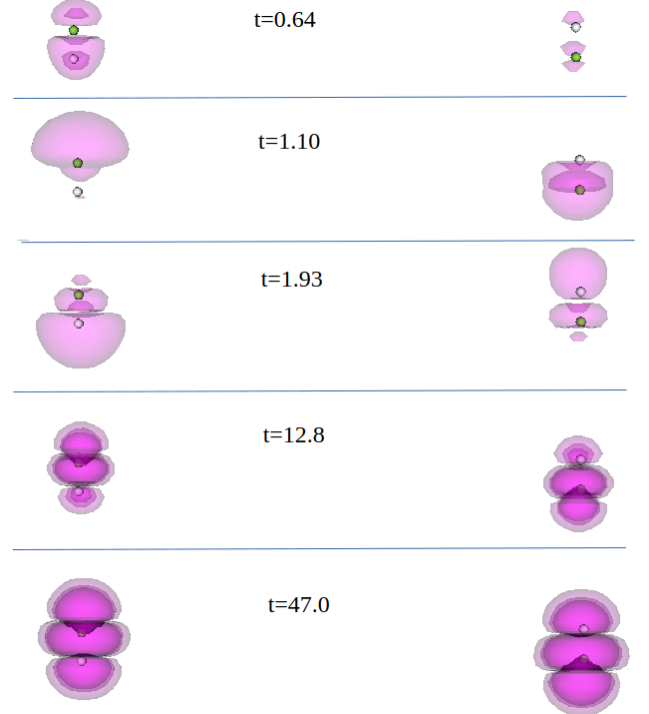


FIG. 10: Snapshots of the charge density difference between the excited state and the ground state for the antiparallel HF molecules. The left molecule is excited with a delta kick perturbation. The three shades of magenta represents values of -0.00003 , -0.00001 , 0.00004 electrons/ Δx^3 ranging from the lightest to the darkest.

exclusively in the first molecule, followed by gradual excitation of the second molecule. Once the second molecule becomes excited, the charge density oscillations on the two molecules occur in opposition to one another, mirroring each other's behavior.

D. Two CO molecules coupled by light

We conducted a similar investigation to that described in the previous section, but using CO molecules instead. Fig. 11 demonstrates that the molecular dipoles align and oscillate synchronously, mirroring the behavior observed for parallel HF molecules. However, both the amplitude and frequency of these oscillations differ compared to the HF case. The photon occupation in the $|1\rangle$ state is higher for CO compared to HF, which can be attributed in part to CO having a greater number of molecular orbitals than HF. Consistent with the HF results, antiparallel CO molecules exhibit dipole oscillations that are out of phase with each other (Fig. 12). Additionally, the dipole oscillation of the initially perturbed molecule remains largely unchanged regardless of whether the molecules are arranged in parallel or antiparallel configurations. The $|1\rangle$ photon state occupation also

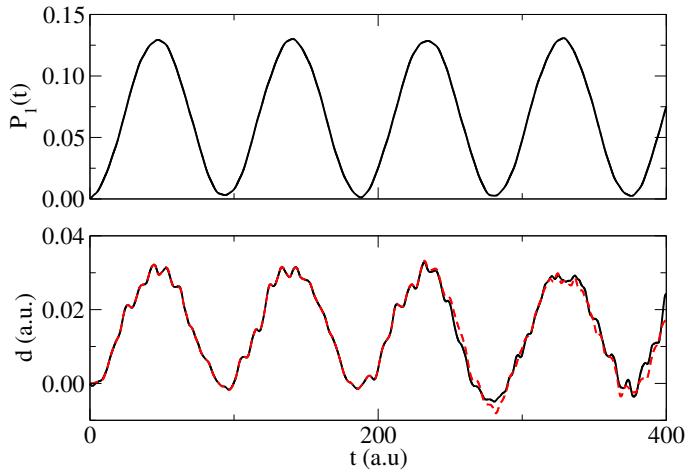


FIG. 11: Occupation of the $|1\rangle$ Fock space and the change of the dipole moment as the function of time when the CO molecules oriented parallel. The solid black line shows the dipole of the molecule which was perturbed by a delta kick excitation, the red dashed line shows the dipole of the second molecule. $\lambda = 0.01$ a.u. and $\omega = 0.467$ a.u. is used in the calculations.

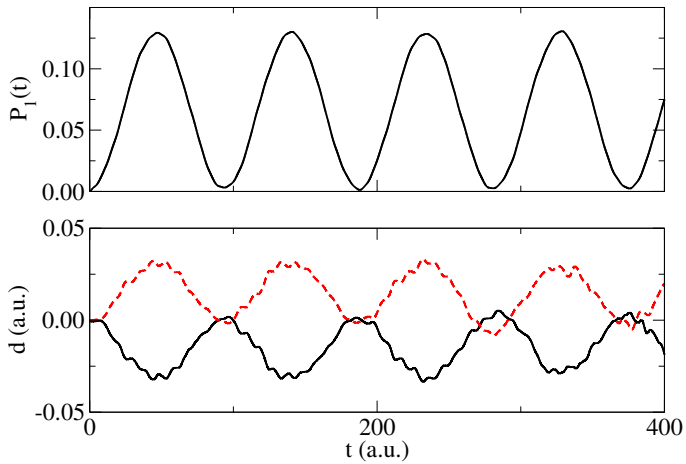


FIG. 12: Occupation of the $|1\rangle$ Fock space and the change of the dipole moment as the function of time when the CO molecules oriented antiparallel. The solid black line shows the dipole of the molecule which was perturbed by a delta kick excitation, the red dashed line shows the dipole of the second molecule. $\lambda = 0.01$ a.u. and $\omega = 0.467$ a.u. is used in the calculations.

E. A CO and a HF molecule coupled by light

In this section, we examine light-mediated coupling between two distinct molecules. The system consists of HF

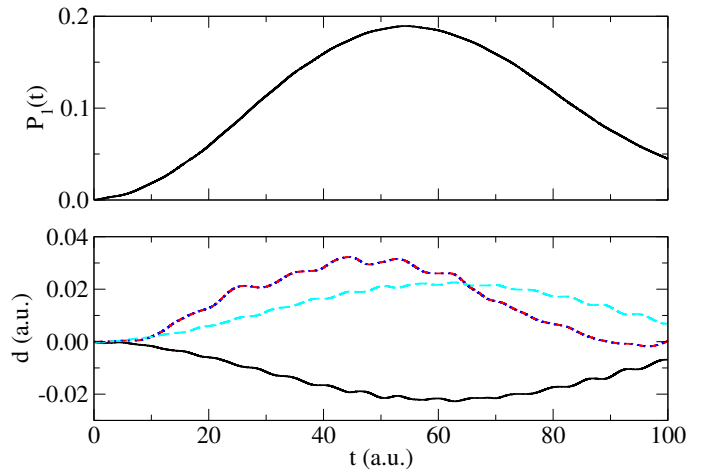


FIG. 13: Occupation of the $|1\rangle$ Fock space and the change of the dipole moment as the function of time. The black solid line represents the time-dependent dipole moment change for the perturbed HF molecule, while the red dashed line indicates the dipole moment change for the unperturbed CO molecule. When the H and F atomic positions are reversed, the long dashed cyan line displays the resulting time-dependent dipole moment change for the perturbed HF molecule, and the dotted blue line shows the dipole moment change for the unperturbed CO molecule (which overlaps with the red dashed line).

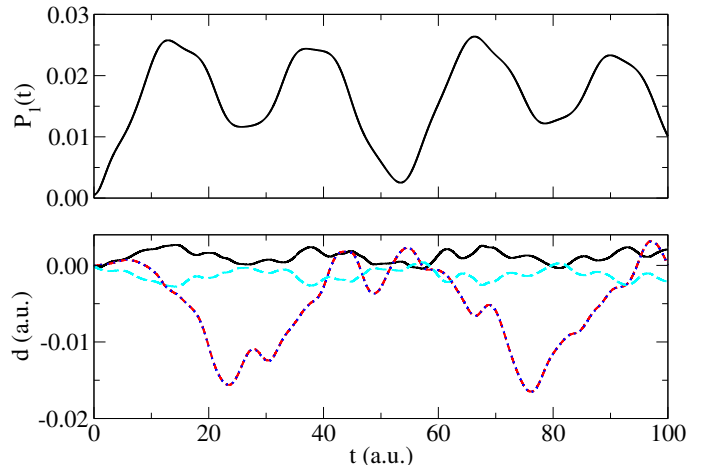


FIG. 14: Same as Fig. 13 but with $\omega = 0.467$ a.u.

and CO molecules with their molecular axes aligned parallel to both the x-axis and the light polarization direction. These molecules are arranged symmetrically about the z-axis, with each positioned at a distance equal to half its bond length from the z-axis. A separation of 30 a.u. between the molecules ensures negligible intermolecular interaction.

A delta kick excitation is applied to an HF molecule, which subsequently induces excitation in a CO molecule.

Fig. 13 displays the time-dependent changes in dipole moments and the occupation of the $|1\rangle$ Fock state. Two calculations are presented: in the first, the F and C atoms are positioned at the top while the H and O atoms are at the bottom; in the second, the H and F atoms are exchanged. This exchange leaves the photon occupation unchanged but symmetrically inverts the dipole oscillation of the HF molecule. The CO molecule's dipole oscillation remains unaffected in both cases. Fig. 14 presents an analogous study with a modified cavity frequency of 0.289 a.u. (compared to 0.467 a.u. used in all previous HF and CO calculations). The qualitative behavior persists: photon occupation remains independent of atomic switching, the CO dipole is unchanged, and the HF dipole undergoes a sign reversal upon switching. However, the oscillation patterns differ markedly—the photon occupation now exhibits four oscillations in the same time period compared to the previous single oscillation, and the dipole moments display increased oscillatory character.

IV. SUMMARY

This work presents a real-time investigation of light-mediated interactions between spatially separated molecules using quantum electrodynamical time-dependent density functional theory based on the Pauli-Fierz Hamiltonian in the velocity gauge. We have developed a first-principles computational framework that combines a Kohn-Sham formulation with a tensor-product representation of electronic real-space orbitals and photonic Fock states, enabling explicit simulation of coupled electron-photon dynamics beyond perturbation theory. The approach employs a consistent single-mode approximation within the dipole regime, retaining both paramagnetic and diamagnetic coupling terms to preserve gauge invariance. Time propagation is performed using a fourth-order Taylor expansion of the time-evolution operator, providing a computationally tractable yet rigorous description while maintaining the favorable scaling of conventional density functional theory.

Our simulations demonstrate a striking contrast between vacuum and cavity environments. For Nitrobenzene, cavity coupling substantially amplifies the dipole response and sustains coherent charge-density oscillations that decay rapidly in vacuum, reflecting modification of the molecular energy landscape through polariton formation. For spatially separated molecular dimers

positioned far beyond the range of direct intermolecular interactions, excitation remains strictly localized in vacuum, with the distant molecule remaining entirely unexcited. In sharp contrast, when both molecules couple to the same cavity mode, the initially excited molecule generates cross-coupling through the photon field, which acts back on the distant molecule. After a transient period, the two molecular dipoles synchronize, oscillating nearly identically and demonstrating coherent energy exchange mediated by the shared quantized field.

The strength and symmetry of cavity-mediated coupling depend sensitively on molecular orientation relative to field polarization. Parallel-aligned molecules exhibit in-phase dipole oscillations, while antiparallel configurations produce out-of-phase oscillations with inverted charge-density dynamics. Perpendicular orientations suppress coupling almost entirely. The photon occupation number and photon coordinate exhibit distinct oscillatory behaviors, with the total energy oscillating synchronously with occupation changes reflecting population redistribution between photon states. The amplitude, frequency, and coherence time of cavity-mediated oscillations vary across different molecular species, reflecting differences in dipole moments, electronic structure, and resonance conditions. These results provide direct evidence that the cavity mode functions as a dynamical communication channel, converting strictly local excitations into collective responses through coherent coupling to the quantized field rather than near-field Coulomb interactions or molecular overlap.

The present work establishes a foundation for exploring several important directions. The tensor-product framework can be scaled to investigate cavity-mediated energy transport in larger molecular assemblies, including molecular crystals and light-harvesting complexes, revealing how excitations delocalize over many emitters via polaritonic channels. Extending the formalism to multimode environments will enable more accurate modeling of experimental platforms and could uncover interference effects and selective energy-transfer pathways. Incorporating dissipation through cavity losses and molecular vibrational coupling will be essential for quantitative comparison with experiments and assessing the robustness of cavity-mediated phenomena under realistic conditions. Exploring alternative excitation schemes beyond delta kicks, such as continuous-wave driving or phase-controlled pulse sequences, could reveal new regimes of molecular synchronization and coherent control.

[1] Francisco J. Garcia-Vidal, Cristiano Ciuti, and Thomas W. Ebbesen. Manipulating matter by strong coupling to vacuum fields. *Science*, 373(6551), 2021.

[2] Michael Ruggenthaler, Nicolas Tancogne-Dejean, Johannes Flick, Heiko Appel, and Angel Rubio. From a quantum-electrodynamical light-matter description to novel spectroscopies. *Nature Reviews Chemistry*, 2(3):0118, Mar 2018.

[3] Johannes Flick, Nicholas Rivera, and Prineha Narang. Strong light-matter coupling in quantum chemistry and quantum photonics. *Nanophotonics*, 7(9):1479–1501, 2018.

[4] Michael Ruggenthaler, Dominik Sidler, and Angel Rubio. Understanding polaritonic chemistry from ab initio quantum electrodynamics. *Chemical Reviews*, 123(19):11191–11229, 2023.

[5] D.N. Basov, Ana Asenjo-Garcia, P. James Schuck, Xiaoyang Zhu, Angel Rubio, Andrea Cavalleri, Milan Delor, Michael M. Fogler, and Mengkun Liu. Polaritonic quantum matter. *Nanophotonics*, 2025.

[6] Thomas W. Ebbesen. Hybrid light–matter states in a molecular and material science perspective. *Accounts of Chemical Research*, 49(11):2403–2412, 2016.

[7] Jonathan J Foley, Jonathan F McTague, and A Eugene DePrince. Ab initio methods for polariton chemistry. *Chemical Physics Reviews*, 4(4), 2023.

[8] Braden M. Weight, Todd D. Krauss, and Pengfei Huo. Investigating molecular exciton polaritons using ab initio cavity quantum electrodynamics. *The Journal of Physical Chemistry Letters*, 14(25):5901–5913, 2023.

[9] Michael Ruggenthaler, Johannes Flick, Camilla Pellegrini, Heiko Appel, Ilya V. Tokatly, and Angel Rubio. Quantum-electrodynamical density-functional theory: Bridging quantum optics and electronic-structure theory. *Phys. Rev. A*, 90:012508, Jul 2014.

[10] Chenzhang Huang, Alexander Ahrens, Matthew Beutel, and Kalman Varga. Two electrons in harmonic confinement coupled to light in a cavity, 2021.

[11] Christian Schafer, Florian Buchholz, Markus Penz, Michael Ruggenthaler, and Angel Rubio. Making ab initio qed functional(s): Nonperturbative and photon-free effective frameworks for strong light–matter coupling. *Proceedings of the National Academy of Sciences*, 118(41):e2110464118, 2021.

[12] Camilla Pellegrini, Johannes Flick, Ilya V. Tokatly, Heiko Appel, and Angel Rubio. Optimized effective potential for quantum electrodynamical time-dependent density functional theory. *Phys. Rev. Lett.*, 115:093001, Aug 2015.

[13] I. V. Tokatly. Time-dependent density functional theory for many-electron systems interacting with cavity photons. *Phys. Rev. Lett.*, 110:233001, Jun 2013.

[14] Michael A. D. Taylor, Arkajit Mandal, Wanghuai Zhou, and Pengfei Huo. Resolution of gauge ambiguities in molecular cavity quantum electrodynamics. *Phys. Rev. Lett.*, 125:123602, Sep 2020.

[15] Javier Galego, Francisco J. Garcia-Vidal, and Johannes Feist. Cavity-induced modifications of molecular structure in the strong-coupling regime. *Phys. Rev. X*, 5:041022, Nov 2015.

[16] Michael A. D. Taylor, Arkajit Mandal, and Pengfei Huo. Light–matter interaction hamiltonians in cavity quantum electrodynamics. *Chemical Physics Reviews*, 6(1):011305, 02 2025.

[17] Peyton Roden and IV Foley, Jonathan J. Perturbative analysis of the coherent state transformation in ab initio cavity quantum electrodynamics. *The Journal of Chemical Physics*, 161(19):194103, 11 2024.

[18] Ruby Manderna, Nam Vu, and IV Foley, Jonathan J. Comparing parameterized and self-consistent approaches to ab initio cavity quantum electrodynamics for electronic strong coupling. *The Journal of Chemical Physics*, 161(17):174105, 11 2024.

[19] Jared D. Weidman, Mohammadhossein (Shahriyar) Dadgar, Zachary J. Stewart, Benjamin G. Peyton, Inga S. Ulusoy, and Angela K. Wilson. Cavity-modified molecular dipole switching dynamics. *The Journal of Chemical Physics*, 160(9):094111, 03 2024.

[20] Braden M. Weight, Xinyang Li, and Yu Zhang. Theory and modeling of light–matter interactions in chemistry: current and future. *Phys. Chem. Chem. Phys.*, 25:31554–31577, 2023.

[21] Péter Badankó, Otabek Umarov, Csaba Fabri, Gábor J Halász, and Ágnes Vibók. Topological aspects of cavity-induced degeneracies in polyatomic molecules. *International Journal of Quantum Chemistry*, 122(8):e26750, 2022.

[22] Giacomo Mazza and Antoine Georges. Superradiant quantum materials. *Physical review letters*, 122(1):017401, 2019.

[23] Omar Di Stefano, Alessio Settineri, Vincenzo Macri, Luigi Garziano, Roberto Stassi, Salvatore Savasta, and Franco Nori. Resolution of gauge ambiguities in ultrastrong-coupling cavity quantum electrodynamics. *Nature Physics*, 15(8):803–808, 2019.

[24] Javier Galego, Francisco J Garcia-Vidal, and Johannes Feist. Cavity-induced modifications of molecular structure in the strong-coupling regime. *Physical Review X*, 5(4):041022, 2015.

[25] Atef Shalabney, Jino George, J a Hutchison, Guido Pupillo, Cyriaque Genet, and Thomas W Ebbesen. Coherent coupling of molecular resonators with a microcavity mode. *Nature communications*, 6(1):5981, 2015.

[26] Florian Buchholz, Iris Theophilou, Soeren EB Nielsen, Michael Ruggenthaler, and Angel Rubio. Reduced density-matrix approach to strong matter-photon interaction. *ACS photonics*, 6(11):2694–2711, 2019.

[27] Christian Schäfer, Michael Ruggenthaler, Heiko Appel, and Angel Rubio. Modification of excitation and charge transfer in cavity quantum-electrodynamical chemistry. *Proceedings of the National Academy of Sciences*, 116(11):4883–4892, 2019.

[28] Lionel Lacombe, Norah M Hoffmann, and Neepa T Maitra. Exact potential energy surface for molecules in cavities. *Physical review letters*, 123(8):083201, 2019.

[29] Arkajit Mandal, Sebastian Montillo Vega, and Pengfei Huo. Polarized fock states and the dynamical casimir effect in molecular cavity quantum electrodynamics. *The Journal of Physical Chemistry Letters*, 11(21):9215–9223, 2020.

[30] Johannes Flick, Davis M Welakuh, Michael Ruggenthaler, Heiko Appel, and Angel Rubio. Light–matter response in nonrelativistic quantum electrodynamics. *ACS photonics*, 6(11):2757–2778, 2019.

[31] Simone Latini, Enrico Ronca, Umberto De Giovannini, Hannes Hubener, and Angel Rubio. Cavity control of excitons in two-dimensional materials. *Nano letters*, 19(6):3473–3479, 2019.

[32] Johannes Flick, Nicholas Rivera, and Prineha Narang. Strong light–matter coupling in quantum chemistry and quantum photonics. *Nanophotonics*, 7(9):1479–1501, 2018.

[33] Francisco J Garcia-Vidal, Cristiano Ciuti, and Thomas W Ebbesen. Manipulating matter by strong coupling to vacuum fields. *Science*, 373(6551):eabd0336, 2021.

[34] Anoop Thomas, Lucas Lethuillier-Karl, Kalaivanan Nagarajan, Robrecht MA Vergauwe, Jino George, Thibault Chervy, Atef Shalabney, Eloïse Devaux, Cyriaque Genet, Joseph Moran, et al. Tilting a ground-state reactiv-

ity landscape by vibrational strong coupling. *Science*, 363(6427):615–619, 2019.

[35] D. Novokreschenov, A. Kudlis, I. Iorsh, and I. V. Tokatly. Quantum electrodynamical density functional theory for generalized dicke model. *Phys. Rev. B*, 108:235424, Dec 2023.

[36] Uliana Mordovina, Callum Bungey, Heiko Appel, Peter J Knowles, Angel Rubio, and Frederick R Manby. Polaritonic coupled-cluster theory. *Physical Review Research*, 2(2):023262, 2020.

[37] Derek S. Wang, Tomas Neuman, Johannes Flick, and Prineha Narang. Light–matter interaction of a molecule in a dissipative cavity from first principles. *The Journal of Chemical Physics*, 154(10):104109, 03 2021.

[38] Tor S. Haugland, Christian Schafer, Enrico Ronca, Angel Rubio, and Henrik Koch. Intermolecular interactions in optical cavities: An ab initio qed study. *The Journal of Chemical Physics*, 154(9):094113, 03 2021.

[39] Johannes Flick and Prineha Narang. Ab initio polaritonic potential-energy surfaces for excited-state nanophotonics and polaritonic chemistry. *The Journal of Chemical Physics*, 153(9):094116, 09 2020.

[40] Johannes Flick, Michael Ruggenthaler, Heiko Appel, and Angel Rubio. Kohn–sham approach to quantum electrodynamical density-functional theory: Exact time-dependent effective potentials in real space. *Proceedings of the National Academy of Sciences*, 112(50):15285–15290, 2015.

[41] Arkajit Mandal, Todd D Krauss, and Pengfei Huo. Polariton-mediated electron transfer via cavity quantum electrodynamics. *The Journal of Physical Chemistry B*, 124(29):6321–6340, 2020.

[42] IV Tokatly. Conserving approximations in cavity quantum electrodynamics: Implications for density functional theory of electron-photon systems. *Physical Review B*, 98(23):235123, 2018.

[43] Nam Vu, Daniel Mejia-Rodriguez, Nicholas P. Berman, Ajay Panyala, Erdal Mutlu, Niranjan Govind, and Jonathan J Foley IV. Cavity quantum electrodynamics complete active space configuration interaction theory. *Journal of Chemical Theory and Computation*, 20(3):1214–1227, 2024.

[44] Vasil Rokaj, Davis M Welakuh, Michael Ruggenthaler, and Angel Rubio. Light–matter interaction in the long-wavelength limit: no ground-state without dipole self-energy. *Journal of Physics B: Atomic, Molecular and Optical Physics*, 51(3):034005, 2018.

[45] Johannes Flick, Michael Ruggenthaler, Heiko Appel, and Angel Rubio. Atoms and molecules in cavities, from weak to strong coupling in quantum-electrodynamics (qed) chemistry. *Proceedings of the National Academy of Sciences*, 114(12):3026–3034, 2017.

[46] Jia-Bin You, Jian Feng Kong, Davit Aghamalyan, Wai-Keong Mok, Kian Hwee Lim, Jun Ye, Ching Eng Png, and Francisco J. García-Vidal. Generation and optimization of entanglement between atoms chirally coupled to spin cavities. *Phys. Rev. Res.*, 7:L012058, Mar 2025.

[47] G. S. Agarwal. Control of the purcell effect via unexcited atoms and exceptional points. *Phys. Rev. Res.*, 6:L012050, Mar 2024.

[48] Matteo Castagnola. Realistic *Ab Initio* Predictions of Excimer Behavior under Collective Light-Matter Strong Coupling. *Physical Review X*, 15(2), 2025.

[49] Millan F. Welman, Tao E. Li, and Sharon Hammes-Schiffer. Light-matter entanglement in real-time nuclear-electronic orbital polariton dynamics, 2025.

[50] Johannes Feist and Francisco J Garcia-Vidal. Extraordinary exciton conductance induced by strong coupling. *Physical review letters*, 114(19):196402, 2015.

[51] Christian Schäfer, Michael Ruggenthaler, Heiko Appel, and Angel Rubio. Modification of excitation and charge transfer in cavity quantum-electrodynamical chemistry. *Proceedings of the National Academy of Sciences*, 116(11):4883–4892, 2019.

[52] David M. Coles, Niccolò Somaschi, Paolo Michetti, Caspar Clark, Pavlos G. Lagoudakis, Pavlos G. Savvidis, and David G. Lidzey. Polariton-mediated energy transfer between organic dyes in a strongly coupled optical microcavity. *Nature Materials*, 13(7):712–719, Jul 2014.

[53] Johannes Schachenmayer, Claudiu Genes, Edoardo Tignone, and Guido Pupillo. Cavity-enhanced transport of excitons. *Phys. Rev. Lett.*, 114:196403, May 2015.

[54] M. Fierz and Wolfgang Ernst Pauli. On relativistic wave equations for particles of arbitrary spin in an electromagnetic field. *Proceedings of the Royal Society of London. Series A. Mathematical and Physical Sciences*, 173(953):211–232, 1939.

[55] W Greiner and J Reinhardt. *Field Quantization*. Springer-Verlag, Berlin, 1996.

[56] Michael Ruggenthaler, Johannes Flick, Camilla Pellegrini, Heiko Appel, Ilya V Tokatly, and Angel Rubio. Quantum-electrodynamical density-functional theory: Bridging quantum optics and electronic-structure theory. *Physical Review A*, 90(1):012508, 2014.

[57] David Parker Craig and Thiru Thirunamachandran. *Molecular quantum electrodynamics: an introduction to radiation-molecule interactions*. Courier Corporation, 1998.

[58] Tor S. Haugland, Enrico Ronca, Eirik F. Kjønstad, Angel Rubio, and Henrik Koch. Coupled cluster theory for molecular polaritons: Changing ground and excited states. *Phys. Rev. X*, 10:041043, Dec 2020.

[59] Johannes Flick, Michael Ruggenthaler, Heiko Appel, and Angel Rubio. Atoms and molecules in cavities, from weak to strong coupling in quantum-electrodynamics (qed) chemistry. *Proceedings of the National Academy of Sciences*, 114(12):3026–3034, 2017.

[60] Rosario R. Riso, Tor S. Haugland, Enrico Ronca, and Henrik Koch. Molecular orbital theory in cavity QED environments. *Nature Communications*, 13(1):1368, March 2022. Publisher: Nature Publishing Group.

[61] Marcus D. Liebenthal, Nam Vu, and A. Eugene De-Prince, III. Equation-of-motion cavity quantum electrodynamics coupled-cluster theory for electron attachment. *The Journal of Chemical Physics*, 156(5):054105, February 2022.

[62] Nam Vu, Daniel Mejia-Rodriguez, Nicholas P. Berman, Ajay Panyala, Erdal Mutlu, Niranjan Govind, and Jonathan J. IV Foley. Cavity Quantum Electrodynamics Complete Active Space Configuration Interaction Theory. *Journal of Chemical Theory and Computation*, 20(3):1214–1227, February 2024. Publisher: American Chemical Society.

[63] Alexander Ahrens, Chenhang Huang, Matt Beutel, Cody Covington, and Kálmán Varga. Stochastic variational approach to small atoms and molecules coupled to quantum field modes in cavity qed. *Phys. Rev. Lett.*, 127:273601, Dec 2021.

[64] Yetmgeta S. Aklilu and Kálmán Varga. Description of the hydrogen atom and the he^+ ion in an optical cavity using the pauli-fierz hamiltonian. *Phys. Rev. A*, 110:043119, Oct 2024.

[65] I. V. Tokatly. Time-dependent density functional theory for many-electron systems interacting with cavity photons. *Phys. Rev. Lett.*, 110:233001, Jun 2013.

[66] Johannes Flick, Michael Ruggenthaler, Heiko Appel, and Angel Rubio. Kohn–sham approach to quantum electrodynamical density-functional theory: Exact time-dependent effective potentials in real space. *Proceedings of the National Academy of Sciences*, 112(50):15285–15290, 2015.

[67] E. Jaynes and F. W. Cummings. Comparison of quantum and semiclassical radiation theories with application to the beam maser. 1962.

[68] Michael A. D. Taylor, Arkajit Mandal, and Pengfei Huo. Resolving ambiguities of the mode truncation in cavity quantum electrodynamics. *Opt. Lett.*, 47(6):1446–1449, Mar 2022.

[69] Felix Benz, Mikolaj K. Schmidt, Alexander Dreismann, Rohit Chikkaraddy, Yao Zhang, Angela Demetriadou, Cloudy Carnegie, Hamid Ohadi, Bart de Nijs, Ruben Esteban, Javier Aizpurua, and Jeremy J. Baumberg. Single-molecule optomechanics in picocavities. *Science*, 354(6313):726–729, 2016.

[70] Cloudy Carnegie, Jack Griffiths, Bart de Nijs, Charlie Readman, Rohit Chikkaraddy, William M. Deacon, Yao Zhang, István Szabó, Edina Rosta, Javier Aizpurua, and Jeremy J. Baumberg. Room-temperature optical picocavities below 1 nm³ accessing single-atom geometries. *The Journal of Physical Chemistry Letters*, 9(24):7146–7151, 2018.

[71] Yuan Luo, Jiaxin Zhao, Antonio Fieramosca, Quanbing Guo, Haifeng Kang, Xiaoze Liu, Timothy C. H. Liew, Daniele Sanvitto, Zhiyuan An, Sanjib Ghosh, Ziyu Wang, Hongxing Xu, and Qihua Xiong. Strong light-matter coupling in van der waals materials. *Light: Science & Applications*, 13(1):203, Aug 2024.

[72] T. Cubaynes, M. R. Delbecq, M. C. Dartialh, R. Assouly, M. M. Desjardins, L. C. Contamin, L. E. Bruhat, Z. Leghtas, F. Mallet, A. Cottet, and T. Kontos. Highly coherent spin states in carbon nanotubes coupled to cavity photons. *npj Quantum Information*, 5(1):47, Jul 2019.

[73] Stefan Blien, Patrick Steger, Niklas Hüttner, Richard Graaf, and Andreas K. Hüttel. Quantum capacitance mediated carbon nanotube optomechanics. *Nature Communications*, 11(1):1636, Apr 2020.

[74] Justin Malave, Alexander Ahrens, Daniel Pitagora, Cody Covington, and Kálmán Varga. Real-space, real-time approach to quantum-electrodynamical time-dependent density functional theory. *The Journal of Chemical Physics*, 157(19):194106, 11 2022.

[75] Marcus Dante Liebenthal and A. Eugene DePrince, III. The orientation dependence of cavity-modified chemistry. *The Journal of Chemical Physics*, 161(6):064109, August 2024.

[76] Marit R. Fiechter and Mark Kamper Svendsen. On the hamiltonian used in polaritonic chemistry, 2025.

[77] John P. Perdew, Kieron Burke, and Yue Wang. Generalized gradient approximation for the exchange-correlation hole of a many-electron system. *Phys. Rev. B*, 54:16533–16539, Dec 1996.

[78] K. Yabana and G. F. Bertsch. Time-dependent local-density approximation in real time. *Physical Review B*, 54:4484–4487, 1996.

[79] Miguel A. L. Marques, Alberto Castro, George F. Bertsch, and Angel Rubio. octopus: a first-principles tool for excited electron–ion dynamics. *Computer Physics Communications*, 151:60–78, 2003.

[80] Kalman Varga and Joseph Driscoll. *Computational Nanoscience: Applications for Molecules, Clusters, and Solids*. Cambridge University Press, Cambridge, 2011.